Chemical Engineering Journal 221 (2013) 146–158

Contents lists available at SciVerse ScienceDirect

Chemical Engineering Journal

journal homepage: www.elsevier.com/locate/cej

# Synthesis and characterization of valonea tannin resin and its interaction with palladium (II), rhodium (III) chloro complexes ☆

Mustafa Can [a,*], Emrah Bulut [b], Ahmet Örnek [a], Mahmut Özacar [b]

[a] Institute of Sciences and Technology, Sakarya University, 54187 Sakarya, Turkey
[b] Department of Chemistry, Sakarya University, 54187 Sakarya, Turkey

## HIGHLIGHTS

- Valonea tannin and formaldehyde condensation reaction was carried to prepare TAR.
- TAR formation and interaction with PGM chloro complexes have been characterized.
- Pd (II) reduced to metallic $Pd^0$ onto TAR.
- TAR–Rh (III) surface complex interaction has been characterized.
- TAR can be applied to recover PGMs efficiently and simply with low cost.

## ARTICLE INFO

*Article history:*
Received 17 November 2012
Received in revised form 11 January 2013
Accepted 12 January 2013
Available online 5 February 2013

*Keywords:*
Valonea
Tannin
Polymer
Polyphenol
Resin
Adsorption
Rhodium
Palladium

## ABSTRACT

Valonea tannin (TA) and formaldehyde condensation reaction was carried out under alkaline condition to prepare the valonea tannin–formaldehyde resol resin (TAR). Obtained resin was used as adsorbent for recovery of palladium (II) and rhodium (III) ions from chloride-containing solutions. This kind of recovery was very simple and useful for generating little secondary wastes. Interaction of adsorption also was investigated: Chloropalladium (II) species were reduced to Pd(0), while hydroxyl groups of TAR were oxidized during the adsorption. Proposed adsorption of the aquachlororhodium (III) species mostly takes place via ligand exchange mechanism. TAR, Rh-adsorbed TAR, and Pd-adsorbed TAR were characterized by scanning electron microscopy, energy-dispersive spectrometry, X-ray diffraction spectroscopy, and Fourier transform infrared–attenuated total reflection spectroscopy.



## 1. Introduction

Because of lower ore reserve and industrial applications, with the exception of the automotive sector is the low amount of use, an important part of the Platinum Group Metals (PGMs) placed on the market provided by on the recycling processes. PGMs are present in the form of chloro-complexes with complicated solution chemistry. The species composition is dependent on factors such as chloride concentration, pH, ionic strength, temperature, and the age of the solution. The formation of metal complexes by PGMs is related to the solution composition. This in turn may affect the adsorption mechanism involved, i.e. chelation rather than ion exchange, and the affinity of the metal species for sorption sites on the adsorbents. Solution chemistry of PGMs are generally very different to that of base metals [1].

Active carbon [2], ion-exchange resins [3–7] and low cost adsorbents [3–5] are suitable for adsorption. Large volumes of published data exist regarding the recovery or removal of base metals from aqueous solutions, but the same cannot be said for precious metal recovery. Published precious metal biosorption data has focused on gold recovery [6,4], but over the last 15–20 years, interest in the recovery of strategically valuable metals such as platinum and palladium has increased [7–9].

Tannins are oligomeric compounds with multiple structure units that have free phenolic groups. Since ancient times it is known that certain organic substances have tanning properties

☆ Funding Sources: This study was supported by the Scientific Research Projects Commission of Sakarya University (Project Number: 2009 50 02 005).

* Corresponding author. Present address: Ministry of Education, Adapazarı İmam Hatip School, 54100 Sakarya, Turkey. Tel.: +90 0264 295 60 41, mobile: 0505 253 21 00; fax: +90 0264 295 59 50.
*E-mail address:* mstfacan@gmail.com (M. Can).

1385-8947/$ - see front matter © 2013 Elsevier B.V. All rights reserved.
http://dx.doi.org/10.1016/j.cej.2013.01.043

and are able to tan animal skins to form leather [10,11]. They range anywhere from 500 to sometimes greater than 20,000 in molecular weight [12,13]. Tannins are usually soluble in water [13,14] except for some with high molecular weight structures. Tannins may protect plants from herbivore and invasion of pathogenic microorganisms due to their antimicrobial and antifungal properties [10]. They represent secondary metabolites widely distributed in various sectors of the higher plant kingdom like in barks, leaves, fruits, galls on plants and wooden sectors. The tannins appear as light yellow to brown or white amorphous powders, loose masses, with a characteristic strange smell and astringent taste [15].

Depending on their chemical structure and properties, tannins are usually divided into four major groups: *Gallotannins*, *ellagitannins*, *complex tannins* and *condensed tannins* [12,10,13]. *Gallotannins* are all those tannins in which galloyl units or their *meta*-depsidic derivatives are bound to diverse polyol-, catechin-, or triterpenoid units. *Ellagitannins* are those tannins in which at least two galloyl units are C—C coupled to each other, and do not contain a glycosidically linked catechin unit [16]. *Complex tannins* are tannins in which a catechin unit is bound glycosidically to a gallotannin or an ellagitannin unit. *Condensed tannins* are all oligomeric and polymeric proanthocyanidins formed by linkage of *C*-4 of one catechin with *C*-8 or *C*-6 of the next monomeric catechin [10,17]. The structural variation amongst tannins is caused by oxidative coupling of neighboring gallic acid unit or by oxidation of aromatic rings [18].

As a typical ellagitannins, Turkish valonea tannins contain a large percentage of hexahydroxy diphenol groups (HHDP, Fig. 1), having the potential to yield a high level of ellagic acid [19,20,10,18]. Ellagitannin's esterified groups with hydroxides of glucose; occurs either bridged between different galloyl groups with covalent bonds, or hexahydroxy diphenol group derivatives [19,21]. Bridged group contains asymmetric centers and this allows a rearrangement of the remaining part of D-glucose [19].

Turkish bearded oak (*Quercus cerris*)'s and Anatolian acorn oak (*Quercus macrolepis*)'s fruit acorn capula (valonea) when extracted with acetone/ethylacetate/water mixture to eliminate the sugar fraction, valonea tannin can be obtained [12]. With hydrolyzing this, a significant amount of ellagic acid, valonic acid dilactone, gallic acid, and their derivatives are acquired [19,20,10]. Structures of these compounds are given in Fig. 1. Valonea tannin contains max 7% moisture, max 2% ash, and max 27% non-tannin substance. Tannins in which extracted from acorns should be containing at least 65% tannin [22,23].

The main constituents of the main commercial valonea tannin are castalagin and vescalagin, positional isomers of penta-hexa-hepta-o-galloyl-β-D-glucose, having molecular weight 950–1250 g/mol [20,24,19,13]. These main components can be rearranged to form dimers, trimers, and oligomers [24,13].

Because of precipitate water soluble proteins, tannins are used as tanning agent. They are also used in dyestuff industry, production of iron gallate ink. Other industrial uses of tannins include textile dyes, and as antioxidants in fruit juices. In medicine, tannin can be used healing for burned place, as astringent, and against diarrhea by using effect of shriveling [10]. Tannins have capable to precipitation of heavy metals and alkaloids with an exception of morphine. This can be used against to mentioned media-induced toxicity [14]. Recently the tannins have attracted scientific interest, especially due to the increased incidence of deadly illnesses such as AIDS and various cancers [25,14].

Ellagitannins, a subclass of hydrolysable plant tannins, are receiving increasing attention as excellent resource for replacing petroleum-derived phenolic compounds [26]. When low molecular weight phenolic in tannins hydrolyzing, they can be easily converted to gallic acid. Likewise, bigger phenolics in the valonea tannin (Fig. 2) produce gallic acid to a large extent. Gallic acid is most frequently encountered in plants in ester forms [14]. Other phenolic acids are also present, but in low proportions. Therefore a biocompatible, and cytocompatible member of polyphenolic polymers that produced from valonea, gallic acid molecule as the smallest repeating structure used as a representative [27].

Conventional syntheses of polyphenol resins are classified into chemical and enzymatic methods [28]. In the chemical methods, phenol reacts with formaldehyde in acidic or alkaline media, forming novolac or resol resins, respectively [6]. As phenolic resins completing their century of existence, they continue to be an important bonding agent with favorable cost/performance

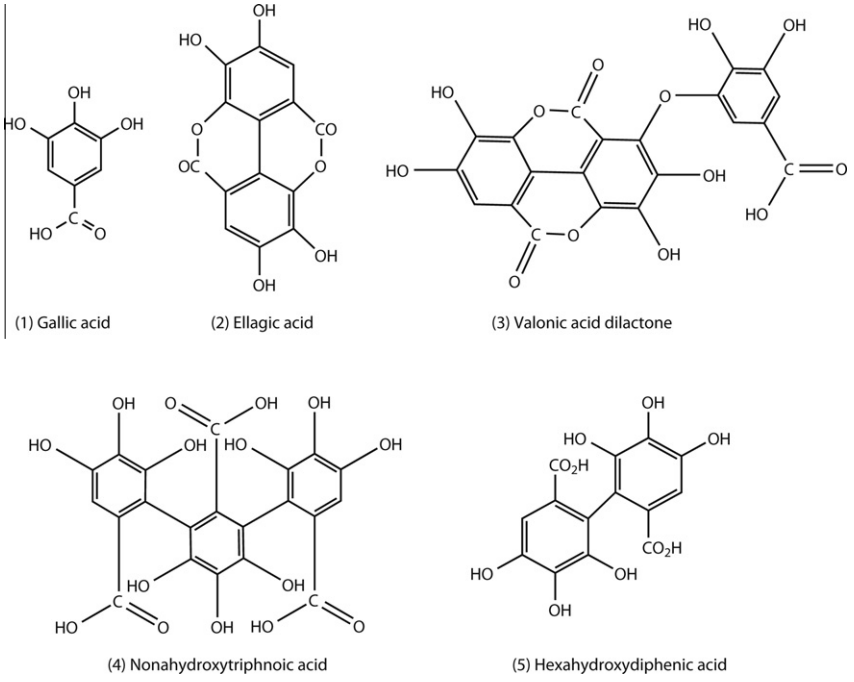


**Fig. 1.** Low molecular weight phenolics of valonea tannin.

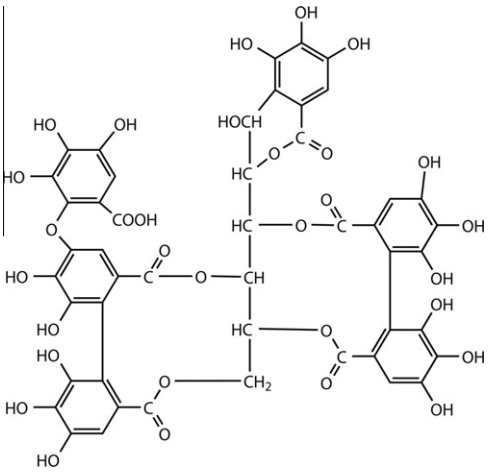

**Fig. 2.** Typical structure of valonea tannin.

characteristics that surpass most other polymeric resins. It is equally important as a resin matrix for fiber reinforced composites requiring fire, smoke, and toxicity characteristics in critical high performance areas such as aircraft interiors/panels, tunnel materials, offshore oilfield grating and deluge pipe, and fire safe components [29]. Adam and Holmes [30] first demonstrated the capacity of this type resins to exchange cations on the very weakly dissociating phenolic groups [31,32]. These can be used for isolating and separating rare alkali metals [33], actinides [34–38], heavy metals [39,32,34,40–44] and, precious metals [45–48].

The increasing demand for the Platinum Group Metals (PGMs) for production of catalysts and in related industries, combined with the limited resources available, has led to increasing interest in the recovery of these strategic elements [49]. Up to now, only a few studies have been carried out on the separation of PGMs using tannin derivatives [50,51,9,46,48].

Recently, studies have begun to focus significantly on the mechanisms involved in the binding of PGM to tannin resin. Initially, these took the form of conjecture, but now spectroscopic methods such as variants of X-ray, and Fourier transform infrared (FTIR) spectroscopies for the elucidation of binding mechanisms are widely used. These methods confirmed that no chemical change to the adsorbent took place after metal loading, suggesting that the acidic conditions merely favored electrostatic interaction between PGM and polyphenolics [47]. FT-IR spectroscopy is a powerful analytical method for monitoring the resin formation and interaction mechanism with PGM. It offers a unique capability in terms of its quantitative measurement of the conversion of a specific functional group. In particular, the appearance of the hydroxyl group, methylol group and dimethylene ether bridges can be easily monitored [26,52]. In addition to using XRD patterns, redaction of PGM can be easily realized from sharp peaks [53,54]. The scanning electron microscopy (SEM) has been used to show the particle size and morphology of these resins. EDX analysis was performed to determine elemental distribution for scanning surface in samples [55].

Secondly, we give a detailed overview of the current information, and studies employed to understand the tannins, and PGM research, this study focused on two main areas. First, investigation of tannin–formaldehyde resol resin (TAR) formation using several techniques such as FTIR, SEM, energy-dispersive spectrometry (EDS), and XRD. Second, interaction characterization of palladium (II) and rhodium (III) ions in chloride containing aqueous solutions onto obtained TAR particles. Our objectives were to reduce the cost, and time while obtaining the starting chemicals from renewable sources.

## 2. Materials and methods

### 2.1. Materials

Commercial valonea tannin extracts were obtained from Tuzla Dericiler Sanayi Sitesi, İstanbul-Türkiye. The extract, which is considered their tannin content, was used in the polymerization experiments without further purification. Valonea is obtained from the acorn cup of the oak which grows in Asia Minor. The tannin content of valonea is about 35%. Turkish oak is a source of valonea where there are two factories having extraction batteries to produce tannin from valonea.

$RhCl_3{\cdot}3H_2O$, $PdCl_2$, $NH_3$, HCOH, $HNO_3$, HCl, NaCl and, NaOH purchased from Merck Company. AAS standard solutions for determination of PGM purchased form UltraScientific Company. All other reagents were analytical grade.

The aqueous Pd (II) stock solution was prepared from solid $PdCl_2$ in 1.0 M $HNO_3$. The aqueous Rh (III) stock solution was prepared from solid $RhCl_3{\cdot}3H_2O$ in 1.0 M HCl. The studied solutions of palladium (II) were obtained by dilution with NaOH or $HNO_3$ to adjust the H+ concentration to the desired value. Moreover, a suitable chloride concentration was obtained. Both of the working stock solutions were prepared to contain 200 mg/dm$^3$ Pd (II) and Rh (III).

### 2.2. Preparation of TAR

The total phenolic content was determined using the Folin–Ciocalteau method, described by Singleton et al. [56]. To 1 g of tannin sample, added at least 60 mL of double distilled water. 5 mL of Folin–Ciocalteau reagent were added. The mixture was then allowed to stand and then 15 mL of a 20% $Na_2C0_3$ solution was added. Final volume was adjusted to 100 mL, and read the color generated after about 2 h at about 25 °C. The absorption was taken at 765 nm against water as blank. The amount of total phenolic is expressed as Gallic acid equivalent (mg Gallic acid/g sample) through the calibration curve of Gallic acid. The total phenolic content of valonea tannin determined as 612 mg/g gallic acid equivalent. When considering the structure of tannins having glucose, this value is approximately 68% tannin content of the commercial valonea extract. These results are in agreement with the Turkish Standards [22], and the Potassium Iodate-test [57].

Commercial valonea extract powder (23.54 g) corresponding to 16 g hydrolysable tannin powder ($14.46 \times 10^{-3}$ mol) was added to 124 mL of 13.3 N (1.33 mol) aqueous ammonia, followed by stirring for 5 min to dissolve it. Solution was heated at 60 °C in boiling flask. The resulting solution was added 130 mL of an aqueous solution containing 37% formaldehyde (1.748 mol), followed by stirring for 5 min for uniform mixing. Immediately after, the temperature is raised to 90 °C. Solution was reacted for 2 h at 90 °C by continuing mixing. Liquid concentrate diluted by adding 100 mL of distilled water. At the end of the production of GAR, the amount of formaldehyde was determined by iodometrically as 5.09 per thousand. This value does not exceed the appropriate limit of 1% [28]. After, brown precipitate containing solution's pH adjusted to pH 2 with $HNO_3$ to remove the residual chemicals. Subsequently, the acid containing solution was filtered and washed with distilled water again. The mixture is allowed to stand after the filtering is done. Finally, TAR resin was dried at 80 °C to thereby obtain an insoluble tannin resin.

### 2.3. Characterization

The contents of Rh (III) and Pd (II) in solutions were analyzed by flame atomic absorption spectrometry (FAAS) (Shimadzu 6701F). FT-IR spectra analysis of resins was performed by Shimadzu IR

Prestige-21 at 1 $cm^{-1}$ resolution. Samples were analyzed in attenuated total reflectance (ATR) mode using ceramic light source, KBr/Ge beam splitter and a deuterated l-alanine triglycine sulfate (DLATGS) detector. The FT-IR spectra analyses of TA, TAR, Rh adsorbed TAR and Pd adsorbed TAR were carried out. The spectra were recorded from 1800 to 700 $cm^{-1}$ (accumulating 25 scans) on sample at room temperature. To eliminate moisture and $CO_2$ interference, background spectra were recorded before analysis of the samples. Later on, it corrected by applying IR solution software's Kubelka–Munk function ATR-correction function. SEM and EDS experiments were carried out on JEOL JSM-6060LV scanning electron microscope operated at 20 kV. The morphology and size of TAR was investigated using SEM. To show the presence of Rh and Pd on the GAR, EDS analysis was performed. To clarify interaction mechanism X-ray diffraction analysis of TAR measured with RIGAKU $D_{max}$ 2200 at a Cu anode producing Kα radiation (40 kV, 30 mA). The specific surface area of the resin was determined with BET nitrogen adsorption using a Micromeritics Flow Sorb 2300.

### 2.4. Adsorption studies

The palladium (II), and rhodium (III) solutions were prepared by diluting stock solutions containing 200 mg/$dm^3$ metal ion in distilled water to 50 mg/L concentrations. 50 mL of metal ion solutions prepared for adsorption experiments and stirred after adding 200 mg TAR particles. The stirring rate was the same for all. All adsorption experiments were carried out in a standard and strictly adhered to batchwise system at 20 °C for 60 min. Only adsorption capacity experiments were carried out by agitating 1 g TAR with 1000 mL of metal solution of the various initial metal concentrations for 180 min (the time required for equilibrium to be reached between metal ions adsorbed and metal ions in solution). The experiments were performed at 300 rpm. The initial pH of the solutions controlled by adding a small amount of HCl, $HNO_3$, NaOH and $HClO_4$. At the end of the adsorption period, 15 mL samples were centrifuged and the solutions were filtered through a 0.45 μm Milipore filter paper to avoid any solid particle in the aqueous phase. Samples were measured using AAS. All the adsorption tests were performed at least twice so as to avoid wrong interpretation owing to any experimental errors.

FAAS calibrated using 0, 4, 12 and 20 ppm standard solution for Rh (III) and 0, 2, 6 and 10 ppm standard solution for Pd (II) in 1 M HCl. Samples diluted to measurement limits for precise results. Amount of adsorbed metal ions was calculated from the concentrations in solutions before and after adsorption process. Results were taken from the average of three scans for each sample.

## 3. Results and discussion

### 3.1. Preparation of TAR

Alkaline-catalyzed (resol) TAR are prepared similar to phenol–formaldehyde resins. Resol resins formaldehyde/phenol (F/P) molar ratio generally higher than 1 [58,28]. It is preferred that when a hydrolysable tannin powder is added to aqueous ammonia of pH 8 or more [12]. When the amount of the tannin powder is less than this pH value, a precipitate will not occur even if formaldehyde is added thereto. It is preferred that a formaldehyde which undergoes a condensation reaction with the TA powder to form a precipitate be added in an amount with which all of the dissolving TA can be precipitated. If the formaldehyde solution is less, the condensation reaction will not proceed sufficiently and TA which does not precipitate will remain. On the other hand, it is possible to select excessive amount of formaldehyde ratio. In this instance, it would be an economically disadvantageous choice. In addition, to determine the most appropriate F/TA ratio for adsorption of PGMs, molar ratio ranging from 1 to 6 different TAR resins produced. This resins, adsorption pre-experiments results shown in Table 1. It can be observed that the optimal F/P is equal to 4. This ratio has been used for subsequent works.

There are two steps leading to formation of TAR: methylolation and condensation reactions as shown in Fig. 3. The first step, methylolation, is an electrophilic aromatic substitution reaction and, consequently, the products obtained will be substituted in *ortho* positions (Fig. 3a). The second step is a condensation reaction. In this moment, two mechanism involve a hydroxymethyl group with either a TA forming methylene linkage (Fig. 3b) or a hydroxymethyl group forming dimethyl ether linkage (Fig. 3c), releasing a water molecule. Although the dimethyl ether linkage transforms methylene linkage by application of heat (Fig. 3d), but a little dimethyl ether bridge still remain in resin because of condensation reaction deliberately stopped [21]. This will be confirming TAR's FT-IR spectra. These are mono- or polynuclear hydroxymethyl phenols which are stable at room temperatures, but are transformed into three dimensional, cross linked, insoluble and infusible polymers by the application of heat [58].

While we expect a linear polymer of polymerization takes place only in positions that at the *ortho*, there is a small amount of dimethyl ether bridges still remain, and this three-dimensional structure will emerge. Although polymerization was occurred in an acidic environment, all dimethyl ether bridges transformed to methylene bridges, in this way a linear polymer can be said to be built [59]. Due to insoluble cross-linked structure of GAR formed by the reaction of GA with formaldehyde show a perfect adsorbent property for the adsorption of PGMs and unwanted compounds from aqueous solutions [49,60].

### 3.2. FTIR spectroscopy studies

Fig. 4 represents the FTIR–ATR normalized spectra of TA, TAR, Pd and Rh adsorbed TAR. The main bands and their assignments in TA are as follows: stretching vibrations of the aromatic ring $\nu$(C—C)/$\nu$(C=C) at 1699, 1683, 1653, 1601, 1574, 1559, 1539, 1516, 1506, 1456, 1447, 1437, 1317, 1101, 1040 and 748 $cm^{-1}$ [61], stretching vibrations of the carboxylic acid $\nu$(CO) at 1695, 1040, and 748 $cm^{-1}$ [26,62], in plane deformation vibrations of the carboxylic acid $d_{ip}$(O—H) at 1175, and 1101 $cm^{-1}$ [62], torsional vibrations of the carboxylic acid $t$(CO) at 748 $cm^{-1}$ [63,52], stretching vibrations of the phenolic group $\nu$(C—OH) at 1539, 1437, 1317, and 1040 $cm^{-1}$ [52], in plane deformation vibrations of the phenolic group $d_{ip}$(O—H) at 1539, 1317, and 1101 $cm^{-1}$, and torsional vibrations of benzene $t$(CH) at 907, 856, and 748 $cm^{-1}$ [52,64]. One argued that, absorption band that much that has been an indication of the complexity of the structure. Assigned spectra peaks presented in Supplementary data and here the

**Table 1**
Effect of F/TA molar ratio to $Pd^{2+}$ capacity ($C_{oTAR}$ = 49.9 mg/L, 0.2 g dry-basis TAR, 20 °C, pCl = 2, pH = 3, $v$ = 50 mL, $t$ = 60 min).

| Resin number | F/GA ratio | $Pd^{2+}$ capacity[a] (mg/g) | % Removal |
|---|---|---|---|
| TAR1 | 1.0 | 9.31 | 74.6 |
| TAR2 | 1.5 | 9.89 | 79.3 |
| TAR3 | 2.0 | 10.26 | 82.2 |
| TAR4 | 2.5 | 10.69 | 85.7 |
| TAR5 | 3.5 | 11.53 | 92.4 |
| TAR6 | 4.0 | 12.03 | 96.4 |
| TAR7 | 4.5 | 11.82 | 94.7 |
| TAR8 | 5.0 | 11.29 | 90.5 |
| TAR9 | 5.5 | 9.89 | 79.3 |
| TAR10 | 6.0 | 9.76 | 78.2 |

[a] Estimated uncertainty = ±1 mg/g.

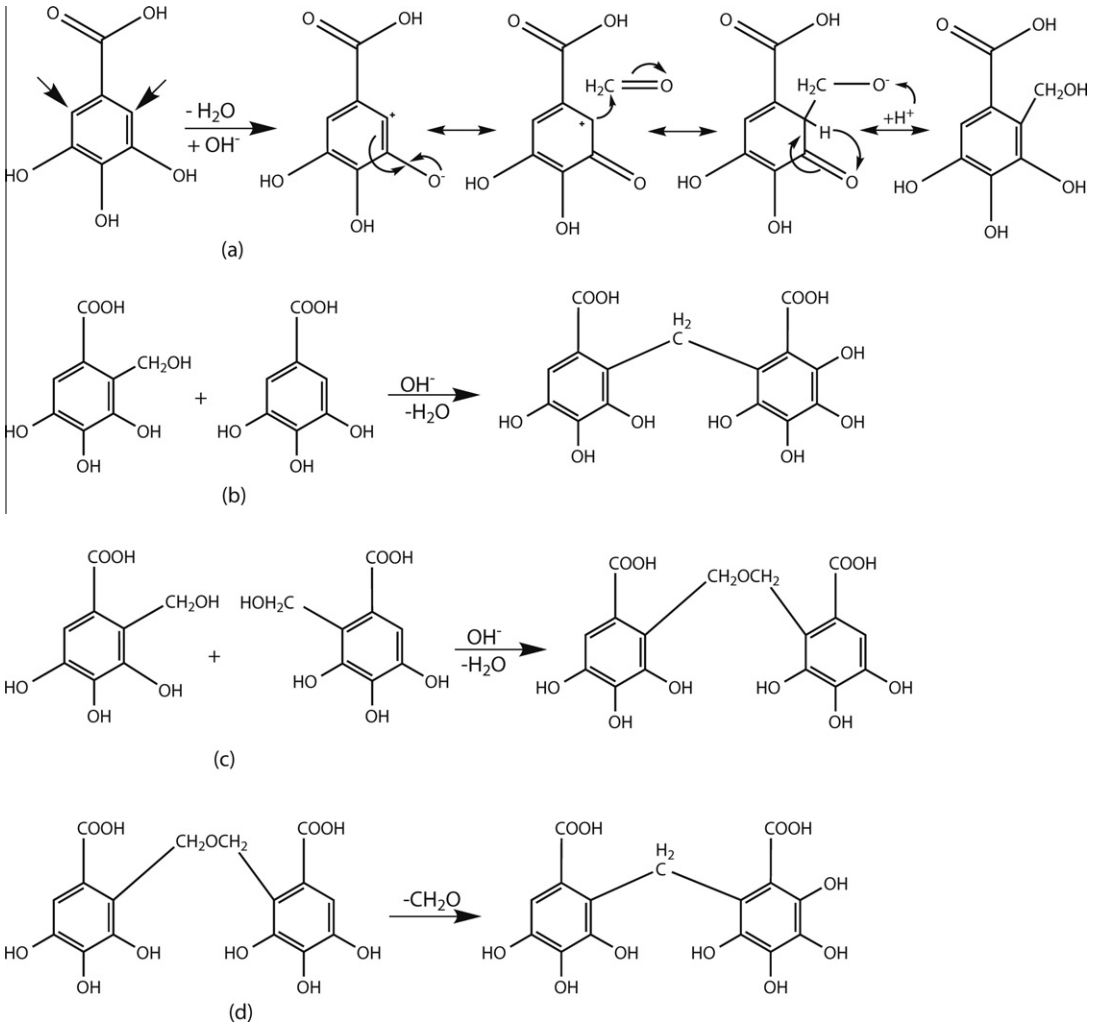


**Fig. 3.** Reaction of TA with formaldehyde. (a) Methylation reaction of TA; (b) formation of methylene bridges in TAR; (c) formation of dimethyl ether bridges in TAR; and (d) transformation of dimethyl ether bridges to methylene bridges.

contribution to IR intensities and frequencies were written highest to lowest.

It is noteworthy that valonea tannin presents a band associated to the carbonyl stretching vibration of ester groups linked to methylene at 1717 $cm^{-1}$ and other one for the modified resin ester group must be linked to an aromatic ring appearing at 1732 $cm^{-1}$ [65]. This adsorption peaks shows valonea tannin contains that free or, boded to glucose gallic acid, ellagic acid, and valonic acid dilactone structures. Disappearing these bans in the TAR spectra can be explained by the hydrolysis (Fig. 5). These groups could be attributed to the hydrolysis of ester groups by heat and acidic conditions of the reaction [13]. As a result of reaction, hexahydroxydiphenic acid and large amount of gallic acid occurs. In the GAR spectra, it is also clear that the presence of a band at 1643 $cm^{-1}$ can be due to the presence of acid groups in the GAR (Fig. 5). Thus, the formation of acid groups in synthesis must be considered.

Formation of TAR leads to obvious changes in FTIR spectra: The new structure consisting of a large molecule that is attenuated many of peaks. Due to participate chemical reaction during formation of TAR, the stretching vibrations between benzene group's carbons peaks at 1699, 1683, 1653, and 1645 $cm^{-1}$ regions showed decrease and shifted to 1643 $cm^{-1}$. In the region above this peaks corresponding to carboxyl–carbonyl groups mentioned before [62]. Small peaks belongs to in plane deformation vibrations of the C—H bond in benzene rings at 1539, 1601, 1437, 1317 $cm^{-1}$ is greatly decreases and some of them disappeared with polymerization [66]. Peaks reflecting $\nu$(C—C)/$\nu$(C=C) and $d_{ip}$(C—H) of the benzene at 1516, and 1506 $cm^{-1}$ regions are disappears, and a new small peak composed to 1505 $cm^{-1}$. 1470, and 1437 $cm^{-1}$ peaks at GA are combined to create peaks at 1454 $cm^{-1}$. Same thing can be said peaks at 1456, and 1446 $cm^{-1}$ regions. A new small peak in spectra of TAR at 1445 $cm^{-1}$, mostly represents benzene ring's $\nu$(CC) and $d_{ip}$(C—H) vibrations. Complete disappearance of the bands at, 1362, 1339, and 1317 $cm^{-1}$ peaks at TA are combined to create broad peaks at 1290–1400 $cm^{-1}$. For TA, a peak reflecting the deformation of the carboxylic acid $d_{ip}$(O—H) group is present at 1175 $cm^{-1}$, as shown in Fig. 4. It can be clearly seen that the intensity of this peak gradually increases and expands, while the peak is slightly shifted to 1217 $cm^{-1}$ in the TAR resin. During the resin formation reaction, Because of hydrolysis reaction occurred, and thus an increase in the amount of the carboxylic acid. The effect of this phenomenon was obvious in the spectra of GAR. The new peak at 1150 $cm^{-1}$ belonged to in plane deformation of OH in COOH and OH groups. 1101 $cm^{-1}$ peak at TA are slightly shifted to create peak at 1103 $cm^{-1}$. This peak mostly representing $\nu$(CO) and $d_{ip}$(O—H) of carboxylic acid groups [66]. 1045 $cm^{-1}$ peak at TA spectra mostly representing $d_{ip}$(O—H) of phenolic and $\nu$(CO) of phenolic and carboxylic acid groups [58,66]. Also, the formation of —$CH_2$—O—$CH_2$— linkage appeared at 1103 $cm^{-1}$. The out of plane deformation

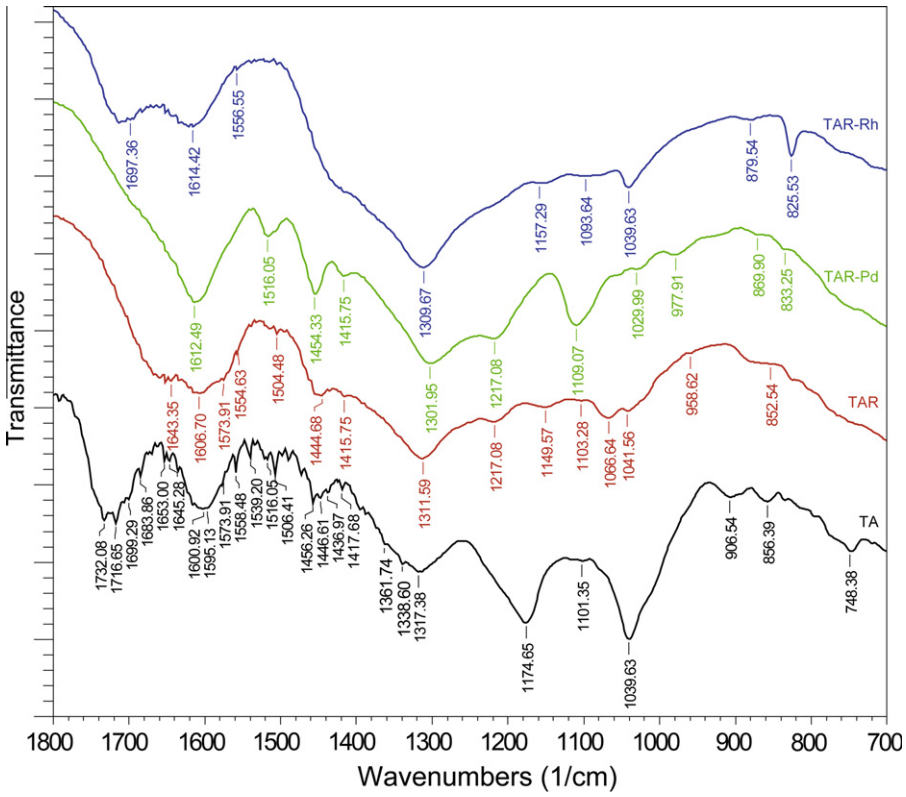


**Fig. 4.** FTIR spectra of TA, TAR, Pd and Rh adsorbed TAR.

vibrations of the C—H bond in benzene rings at 907, 856, and 748 $cm^{-1}$ are completely disappeared due to polymerization [66]. In addition to the same reason vibrations at 907 and 748 $cm^{-1}$ disappeared too.

1539, 1437, 1362, 1339, 1317, 1101, and 1040 $cm^{-1}$ peak mostly representing $d_{ip}$(O—H) of phenolic groups [66,58,67]. Some of them completely disappeared; some of them still remains but combined other peaks in TAR spectra. Despite the use of phenolic OH groups of during the formation of resin, 1445, 1416, 1311, and 1150 $cm^{-1}$ peaks indicate that TAR contains OH groups. These groups can interact with PGM ions and this clearly seen at TAR-Pd and TAR-Rh spectrum (Fig. 4).

1217 $cm^{-1}$ peak mostly representing $d_{ip}$(O—H) of carboxylic acid [64]. Also, the formation of dimethyl ether bridges (—$CH_2$—O—$CH_2$—) appeared a new peak at 1103 $cm^{-1}$ at TAR spectra. Since the most characteristic absorption of aliphatic ethers is a strong band in the 1150–1085 $cm^{-1}$ region due to asymmetrical C—O—C stretching, this band usually occurs about 1050 $cm^{-1}$ region [52,58,26,62]. Therewithal peaks at 1067, and 1042 $cm^{-1}$ in TAR spectra corresponded to single bond (C—O) stretching vibrations of (—COOH) group [68,62].

When the spectra of TAR were compared with the IR spectrum of the TA, the peak intensities at 1574, 1559, 1539, 1516, 1506, 1456, 1447, 1437, and 1417 $cm^{-1}$ was reduced and shifted to 1505,1445, and 1416 $cm^{-1}$ creating weak peak due to the formation of methylene bridges (—$CH_2$—) [58,26,63]. One could suggest that intensity weakening of spectrum, has been indication of becoming big structure. Although, TA was soluble in water, the solubility of TAR was measured to achieve resistant under adsorption conditions. Different curing times have been carried out. Pre-experiments showed that 2 h enough time for resistant [12]. The out of plane deformation vibrations of the (C—H) bond in the benzene rings give absorption bands in the 907–748 $cm^{-1}$ range (Fig. 4, TA). These bands can be used to monitor degree of crosslinking [69]. Majority of these bands disappeared during the process of polymerization; therefore, these behaviors are attributed to the difficulty of phenolic ring deformation when it is highly cross-linked [69,70,67]. In this manner, indicates the formation of insoluble cross-linked structure. Considering all of these, proposed TAR structure shown in Fig. 5. The functional groups before and after adsorption on TAR and the corresponding infrared absorption bands are shown in Supplementary data. The spectra display a various absorption peaks, confirming structure of TAR.

As can be seen the interaction between the TAR and both of metal ion engaged from phenolic groups of TAR. The changes in 1574, 1555, 1150, 1103, and 1067 $cm^{-1}$ wave numbers with the realization of adsorption provide us evidence. These band shifts indicated that the bonded —OH groups play a major role in Pd (II) and Rh (III) sorption on TAR. Here, the main problem is determining of the type of interaction. To reveal that, it would be useful to use instrumentation like XRD and EDS. Disappearing 1573, 1555, 1150 and 1067 $cm^{-1}$ and shifting peaks at 1445, 1312, 1103–1454, 1301, and 1109 in spectra TAR–Pd are evidence of oxidizing hydroxyl groups of TAR to quinone carbonyl groups [71–73]. Increasing peak intensities at 1445 and 1416 $cm^{-1}$ in palladium adsorbed TAR spectra, has been another indication of engaging the quinone structures. In other words, —OH groups oxidized to C=O during adsorption. When TAR–Rh spectra compared to TAR–Pd, band intensities are higher because of the Rh (III) ions adsorbed less than Pd (II) ions. Even if shifted, presence of the bands 1555, 1150, and 1067 $cm^{-1}$, it is also an evidence for more phenolic structure moieties on TAR still remain [66,65,70]. Possible interaction between rhodium chloro aqua complexes and TAR may be surface complex formation. It should be noted here, because of all of the —OH groups in TAR do not participate reaction between TAR and metal ions, some bands appeared in spectrums. When the spectra of Rh and Pd adsorbed TAR were compared with the spectrum of the TAR (Fig. 4), in particular to TAR–Pd spectra, many small peak

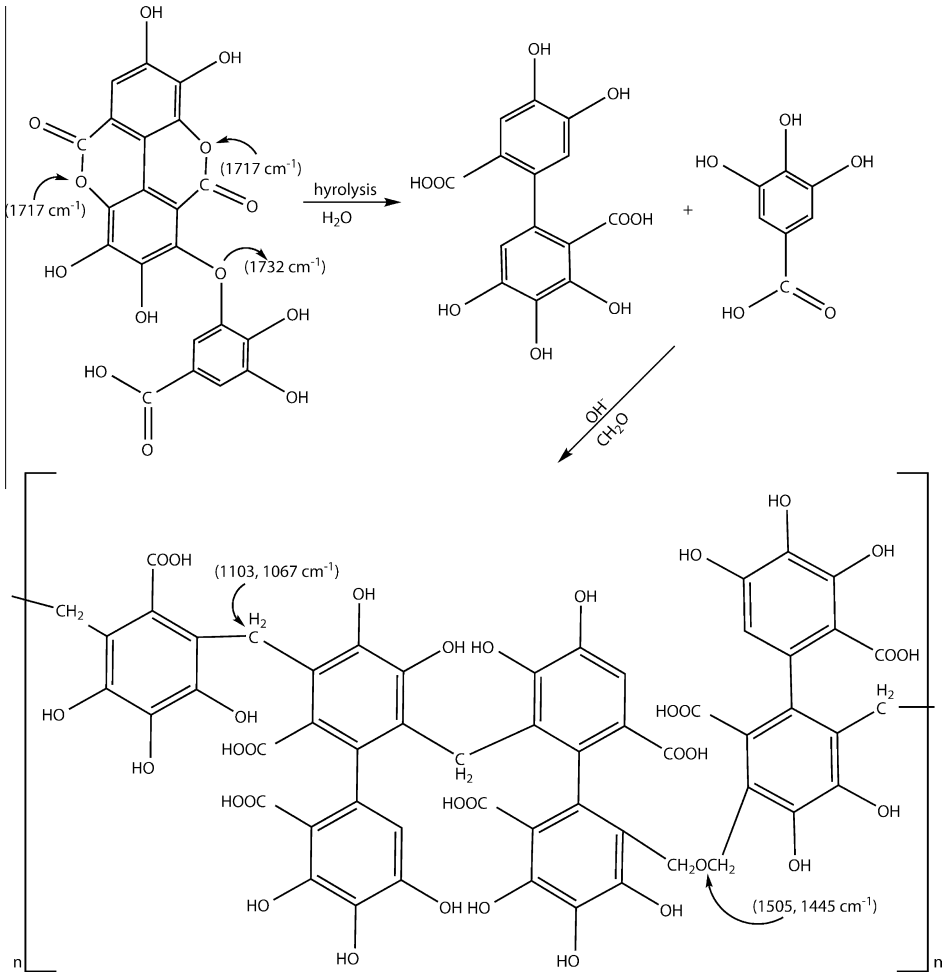


**Fig. 5.** Structure of TAR.

series disappeared. In general it may be argued, proportionally to the degree of adsorption caused to reduction of degree of freedom [26,52].

1217 and 1103 $cm^{-1}$ bands in FTIR spectra of TAR–Pd remained with slightly shifting after adsorption. Due to appearing carboxylic acid's (O—H) bond in plane deformation at these bands showing that carboxylic acid in structure did not interact with the Pd (II) ions. When FTIR spectra of TAR–Rh concerned, these bands increased their intensity contrary to TAR–Pd showing that carboxylic acid in structure interacted with the Rh (III) ions. From the FTIR results of TAR, bands at 1067 and 1042 $cm^{-1}$ have been also an evidence for existence of dimethyl ether bridge (—$CH_2$—O—$CH_2$—) moieties [52,58,26].

### 3.3. Adsorption studies

It can be said that, each kind of Pd (II) and Rh (III) species that in $Cl^-$ ion containing aqueous solutions do not interact with TAR particles. The adsorption capacity and adsorption rate of palladium onto the TAR particles depend on the distribution of Pd (II) and Rh (III) species because the adsorbabilities of species differ from each other due to their different chemical structure [6]. It was reported that the sorption amount and mechanisms are influenced by speciation of palladium; the Pd cationic species ($PdCl^+$, $Pd^{2+}$) and nonionic form ($PdCl_2$) are more favorable than anionic species ($PdCl_4^{2-}$, $PdCl_3^-$) [1,73,74,8]. While, low chloride concentration ($10^{-3}$ M) was especially chosen since the favorable species may occur in this condition [74]. Table 2 shows influence of pH on Pd (II) adsorption under the conditions of $[Cl]_{total}$ 0.001 mol/L. As shown in the Table 2, experimentally highest adsorption efficiency has been achieved at pH = 3. Under these conditions, to determine the distribution of Pd species, computer software Hydra & Medusa [75] used. Fig. 1 in Supporting data, showing that $Cl^-$ concentration is a key parameter for the distribution of Pd species. When $[Cl]_{total}$ is 0.001 mol/$dm^3$, distribution of palladium species as follows: 75% of $PdCl_2$, 20% of $PdCl^+$, 2% of $PdCl_3^-$, 1% of $Pd(OH)_2$, 1% of $Pd(OH)^+$, and 1% of the others. This result indicates that the predominant Pd species are $PdCl_2$ and $PdCl^+$ under these conditions. Both of these occupies species 95% of $[Pd^{2+}]_{total}$ which means that nonionic and cationic Pd (II) species predominate in the aqueous solution rather than anionic species.

**Table 2**
Influence of pH on Pd (II) adsorption and its relationship between the amount of generated hydrogen ions ($C_{oTAR}$ = 49.9 mg/L, 0.2 g TAR, 20 °C, pCl = 3, $v$ = 50 mL, $t$ = 60 min).

| $pH_0$ [a] | $pH_{final}$ [a] | Adsorbed Pd (II) [b] (mg/g) |
|---|---|---|
| 1.99 | 1.98 | 8.75 |
| 2.52 | 2.48 | 10.57 |
| 3.04 | 2.90 | 12.32 |
| 3.54 | 3.21 | 11.81 |
| 3.98 | 3.37 | 11.28 |
| 4.46 | 3.46 | 10.58 |
| 5.01 | 3.49 | 9.96 |

[a] Estimated uncertainty = ±0.05,
[b] Estimated uncertainty = ±1 mg/g.

Moreover it was difficult to estimate the accurate adsorption amount only by TAR particles with initial pH 3, because in course of time some of the Pd species becoming insoluble and, remaining in aqueous solution as suspension. To reduce this, palladium stock solution prepared in 1 M $HNO_3$ and then working pH was adjusted immediately before experiment. Thus, before the deposition of insoluble palladium species, adsorption has begun. It is evident that protons formed during the adsorption low values of the pH. However, decreasing the amount of palladium in the solution must be considered. When all of these are considered, insoluble palladium species will begin to transform into soluble species. The hydrolysis of palladium was observed experimentally at the initial pH 3, by blank test performed which stirring at same conditions without containing TAR particles. The results suggest that the adsorption mechanism was not homogeneous in this initial pH. It was also observed that the pH of the solution was reduced during the adsorption of Pd (II) onto TAR particles (Table 2). This change is attributed to the hydrogen ions releasing from the poly(hydroxyphenol) groups of TAR.

When looking at the literature, Pd (II) adsorption studies with condensed tannin and nitrogen functional group containing resins, optimum pH which highest adsorption efficiency is around 2 [1,8,76,73]. In another study, Wang et al. [46] discuss in Pd (II) sorption on hydrolyzed tannin in hydrochloric acid solutions. Optimum pH for adsorption capacity 5.6, they reported. Note that, at this condition high amount of solid crystal palladium species take place. Adsorption takes place with precipitation on resin surface. Two studies made with hydrolyzed tannin by Ma et al. [9] and Kim and Nakano [73] this value reported as 3. This value in safe region that not been precipitation of palladium species.

When Rh (III) ions are concerned, the situation little more complicated. Water molecules participate to the complex structure by the time and this occurs more than palladium complexes [77]. And with a relatively large rhodium aqua Rhodade complexes, make adsorption harder. To avoid this negative influence, the experiments can be made at the higher pH [78,2,79]. In addition, in order to eliminate the water molecule's effect, $Cl^-$ ions should be used. In this way, relatively small complexes should be involved. Consider, at the higher HCl concentrations, TAR particles beginning to dissolve. Moreover, too high HCl concentrations are changing TAR crystallinity and thus reduce the accessibility to that the acid changes the shape of the adsorption internal sites [80]. Given all these, the most appropriate media for Rh (III) adsorption is aqueous solution containing 1 M HCl. In these conditions, Rh (III) species exist in $[RhCl_6]^{3-}/[RhCl_5H_2O]^{2-} > 1$ concentration ratio [79,81]. Furthermore a new study by Gerber et al. [77] was reported that in 1.0 mol/L HCl the abundance of the $[RhCl_5H_2O]^{2-}$ species is only 8–10% of the total, far from the 70–80% as previously proposed reports. Nonetheless adsorption experiments performed in 1 M HCl containing solutions for due to the aforementioned negative factors. Consequently, it can be said that Rh (III) is most difficult adsorbent in Platinum Group Metals [2,77].

Fig. 2 in Supporting data, shows effect of contact time to adsorption of Pd (II) and Rh (III) ions. The plateau of the plots at higher metal concentrations, suggesting the fact that adsorption has peaked out. The adsorption capacity of TAR particles with respect to Pd (II), and Rh (III) were determined as 87.10, and 10.86 mg/g, respectively. Langmuir single layer adsorption capacity of TAR was found to be 74.43 mg Pd (II)/g and 97.51 mg Rh (III)/g (calculations will be in a subsequent paper). Here, rhodium ions needing more contact time and this may be attributed to big aqua chloro rhodium complexes. In our previous report that has been conducted with having similar structured gallic acid–formaldehyde resin adsorption capacity was determined 99.45 mg Pd (II)/g and 25.12 mg Rh (III)/g [48]. Pyrogallol–formaldehyde nano-resin produced for rhodium adsorption and maximum uptake gained as 15.43 mg Rh (III)/g [82].

Immobilized tannin has also been studied as a Pd (II) adsorption [9]. The adsorption capacity tannin membrane was 27.5 mg/g at 313 K. Condensed-tannin gel particles with poly-hydroxyphenyl groups were synthesized as the adsorbent for the new recovery system of palladium by Kim and Nakano [73]. The loading capacity was approximately 45 mg/g under the conditions of initial pH 2, $[Cl_{tot}]$ 0.012 mol/dm$^3$ at 313 K. Uheida et al. [76] carried out the maximum loading capacity Pd (II) and Rh (III) was determined to be 8.10 and 6.28 mg/g, respectively. In their other work [83], these values were reported as for Pd (II) and Rh (III) to be 10.96 and 15.22 mg/g, respectively. The maximum adsorption capacity of the murexide functionalized halloysite nanotubes adsorbent at optimum conditions was found to be 42.86 mg/g for Pd (II) [84].

Fungal, phenolic polymers and melanins possess many potential metal-binding sites with oxygen-containing groups including carboxyl, phenolic and alcoholic hydroxyl, carbonyl and methoxyl groups being particularly important. Liu et al. [85] were used *Bacillus licheniformis bacteria for biosorption Pd (II). Maximum uptake gained as 224.8 mg/g.* The yeast *Saccharomyces cerevisiae* has been found capable of sorbing palladium ion [86]. *S. cerevisiae* was immobilized using polyethyleneimine and glutaraldehyde to produce a suitable sorbent, capable of high platinum uptake 170 mg/g at low pH (<2). Tu et al. [87] showed the adsorption capacity of the activated carbon having chemically modified with ethyl-3-(2-aminoethylamino)-2-chlorobut-2-enoate as 92 mg/g from solution of pH 1. Polyallylamine hydrochloride-modified *Escherichia coli* biomass was investigated for the removal and recovery of Pd (II) [88]. Maximum uptake of Pd (II) were 265.3 mg/g at pH 3. A feasibility study was performed on Indian almond leaf biomass (*Terminalia catappa* L.) to remove palladium (II) ion from aqueous solution by Ramakul et al. [89]. The maximum biosorption capacity of *T. catappa* L. biomass for Pd (II) ion was 41.86. Sari et al. [90] used moss (*Racomitrium lanuginosum*) biomass and they determined biosorption capacity of the biomass for Pd (II) to be 37.2 mg/g at pH 5. In another study using chitosan derivatives sorption performance has been enhanced by modification of chitosan through the grafting of sulfur compounds (thiourea, rubeanic acid). Sorption capacity gained as *352 mg/g for Pd (II)* [91]. Glutaraldehyde crosslinked chitosan was studied for palladium sorption which has been 180 mg/g maximum Pd (II) capacity [74]. Another modified chitosan resin reported in which modification with glycine modified [92]. The maximum adsorption capacity was found to be 120.39 mg/g. When modification conducted by l-lysine, this value was to be 109.47 mg/g [93]. A method for the synthesis of chitosan crosslinking 2,5-dimercapto-1,3,4-thiodiazole adsorbent was studied by Li et al. [94]. According to this study, it was found that the adsorption capacity was significantly affected by the solution pH, with optimum pH value of 2.0, the saturated adsorption capacity was 16.2 mg/g for Pd (II). The adsorption of Pd (II) on thiourea-modified chitosan microspheres was investigated [95]. The maximum adsorption capacity of 112.4 mg/g for Pd (II) and this value decreased with temperature increasing. As seen above, only a few study reported with tannin resins. And in these articles there has not been rhodium as adsorbent. Also majority of biosorbents has been biomasses and chitosan. Looking at all of these studies, TAR particles can be use efficiently for removal of Pd (II) and Rh (III) from chloride containing aqueous solutions.

### 3.4. Characterization

A typical SEM microimages of Pd (II)- and Rh(III)-adsorbed powder samples of GAR are shown in Fig. 6. These micrographs reveal the homogeneous nature of surface morphology of the TAR powders which also shows that TAR particles possess to porous structure (Fig. 6c). With this porous structure, Pd (II) ions adsorbed to

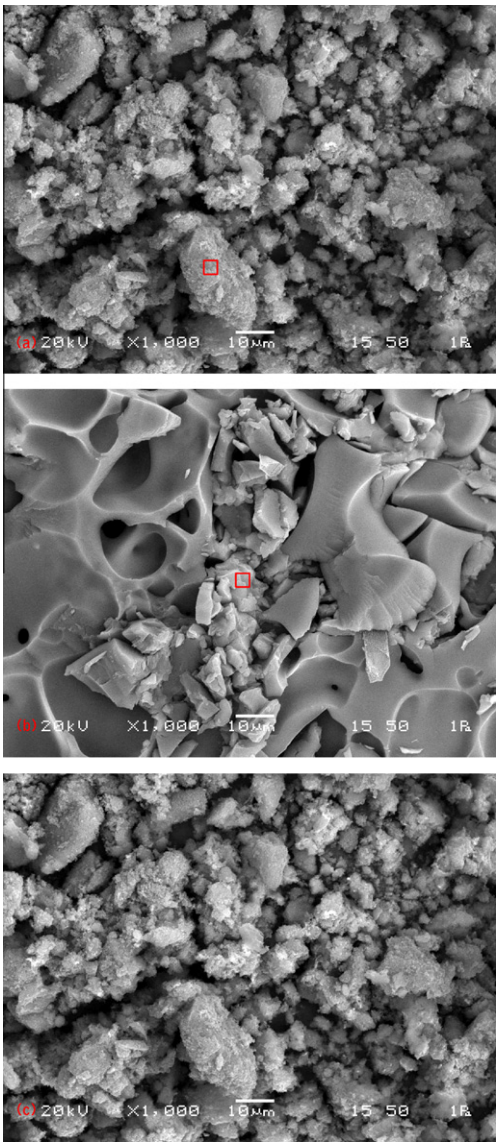


**Fig. 6.** SEM micrograph of Pd (II) adsorbed (a) and Rh (III) adsorbed (b) and natural (c) TAR particles.

the surface, later on they can move into the interior of the pore. This also increases adsorption capacity. The porous structure of TAR is partially disrupted during Rh (III) adsorption in 1 M HCl solution (Fig. 6b). This is contrary to the previous situation, decreases adsorption capacity because of reduction of pores in structure.

The EDS patterns of Pd (II) and Rh (III) adsorbed TAR was given in Fig. 7. EDS analysis did not provide us precise information about exact metal binding mechanism on the surface, but it also provide us ability to make supportive comparisons and taking place of the adsorption. However, when two EDS analysis considered, the weight percentage of Pd was greater than Rh. As the expected result, Rh (III) adsorption capacity on TAR particles showed less than Pd (II) ions. Another important point to note here, suggest us about nature of adsorption mechanism.

In the EDS pattern of Pd at Fig. 7a, palladium and chlorine occurs on surface 2.92%, 0.37%, respectively. This chlorine may only exist made a complex with Pd on the surface of TAR particles. Therefore, at the end of adsorption period, it must be only small amounts of palladium existing on surface as surface complex formed. Probably, large amount of palladium reduced to metallic form with TAR particles. This situation can be proved from XRD pattern at Fig. 8a. When compared to Pd (II) and Rh (III) EDS spectra (Fig. 7), the percentages are respectively 2.92% and 0.33% of the surface. The percentage of $Cl^-$ ions is 2.92% and 0.33%, respectively, too. Despite the adsorption conditions being different, presence of a very small amount of rhodium against chlorine (when converted to molar ratio), it can be explained by Rh (III) complexed with $Cl^-$ ions on TAR surface. This shows, Rh (III) adsorption stage is surface complex formation. Once and for all XRD pattern results (Fig. 8) will help us to make a final decision on this issue.

Specific surface area (BET) and the total pore volume measurements of TAR particles are 8.07 $m^2/g$. This value when compared to other phenolic resin [48] has been lower, and this suggested that it's low adsorption capacity.

### 3.5. Adsorption mechanism

The schematic diagram shown in Fig. 9 illustrates the adsorption mechanisms of Pd (II). The adsorption of Pd (II) follows two steps; firstly, surface complex formation takes place between the TAR particles and chloro palladium species (Fig. 9a). Secondly, while palladium complex reducing to metallic form (Pd0), hydroxyl groups of TAR oxidized to quinone carbonyl groups (Fig. 9b).

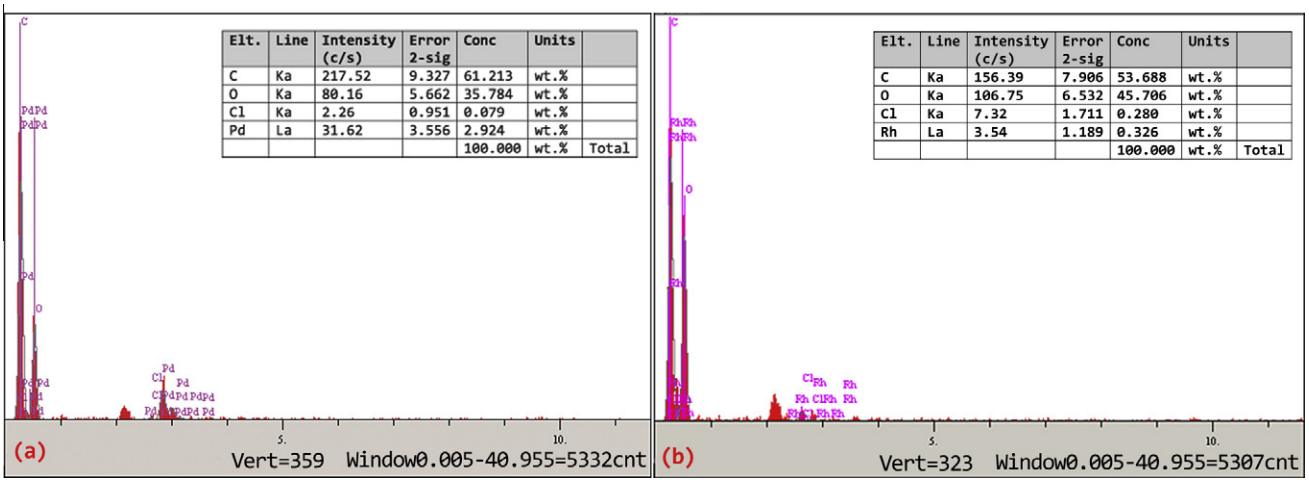


**Fig. 7.** Energy dispersive spectroscopic analysis (EDS) of pattern of Pd (II) adsorbed (a) and Rh (III) adsorbed (b) TAR (20 kV, scattering angle: 35°, measuring time: 10 s).

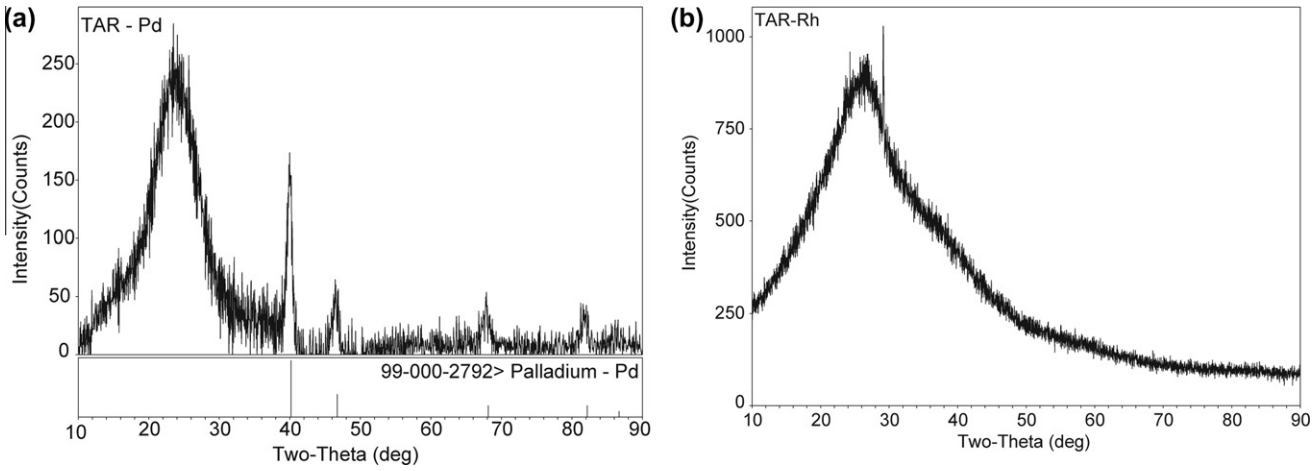


**Fig. 8.** XRD pattern of (a) palladium and (b) rhodium adsorbed TAR particles. Vertical lines represent the XRD peaks of metallic palladium ($Pd^0$).

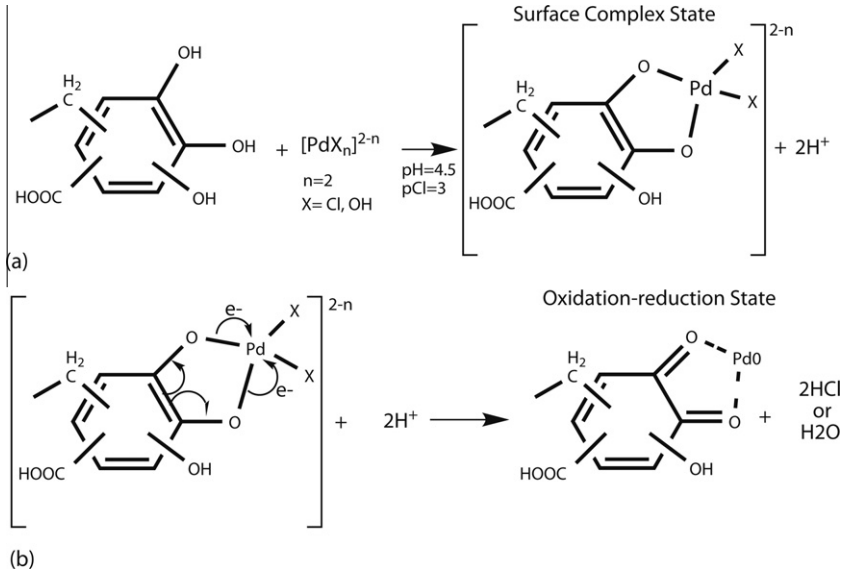


**Fig. 9.** Adsorption mechanism steps of Pd (II): (a) surface complex formation and (b) oxidation–reduction reactions between $PdX_2$ and adjacent hydroxyl groups of TAR.

The generation of $Pd^0$ on the TAR after the adsorption was elucidated by XRD diffractogram shown in Fig. 8a. The five peaks at $2\theta$ = 39.98, 46.44, 68.38, 82.27, and 86.96, which definitely belong to elemental crystalline palladium verifying the reduction of Pd (II) to $Pd^0$. This suggests Pd (II) underwent subsequent reduction after being adsorbed onto TAR surface [72,46,73,8]. In a study Parajuli and colleagues [96], only one OH bonded to benzene chain phenolic resin cannot reduce Pd (II). But, when Au (III) is concerned situation is reversed. In here, our resins owing to having two or more OH groups that bonded to benzene ring and this providing to TAR stable quione structures reduction of palladium can be possible. As mentioned above, disappearing 1643, 1574, 1555, 1150, and 1067 $cm^{-1}$ and shifting peaks at 1454, 1321, and 1103–1454, 1302, and 1109 $cm^{-1}$. TAR–Pd spectra may also explain the oxidation hydroxyl groups of TAR to quinone carbonyl groups.

As shown in Table 2, pH decreases due to the hydrogen ions released from TAR. The amount of generated hydrogen ions was plotted against the adsorbed amount of palladium between at the initial pH 2, and 5, as shown in Fig. 3 at Supporting data. The slope elucidates that the release of two hydrogen ions results in the reduction of one Pd (II) through two electron transfer from TAR to Pd species. Mentioned these results, support proposed mechanism that has been showing at Fig. 9.

The schematic diagram shown in Fig. 10 illustrates the adsorption mechanisms of Rh (III). The adsorption of Rh (III) follows the ionization and adsorption model. When there is an absence of the phenolic and acidic groups, the π sites in the carbons of the benzene chain play an important role in $[RhCl_6]^{3-}$ ions (or $[RhCl_5H_2O]^{2-}$) adsorption on the TAR surface. According to this model, in strong acid concentrations, a large amount of $H_3O^+$ was firstly adsorbed in the π sites [97]. These sites could be the π sites, which are capable of acting as the electron donors (as a Lewis-type acid) to form a coordination bond with anionic aqua chloro complexes of Rh (III) in which acts as a Lewis-type base. Subsequently, slow intra molecular transformation of the latter to an inner sphere complex. As the slow intramolecular conversion reaction (the postulated rate-limiting step) apparently occurs away from the interface [98]. Due to carbons of benzene, bonded groups to such as carboxyl, C—C bond, dimethyl ether, and methylene, a relatively small amount of free π site carbons located at TAR molecules [99], and this decreased to the adsorption capacity when compared to similar resin in our recent study [48]. Accordingly, the metal complex attached decreasingly to the free π site carbons of surface through an electrostatically held proton. Another reason for being capacity lower, it may be presence of large amount of oxygen attached to benzene ring. The presence of the surface oxygen groups near these

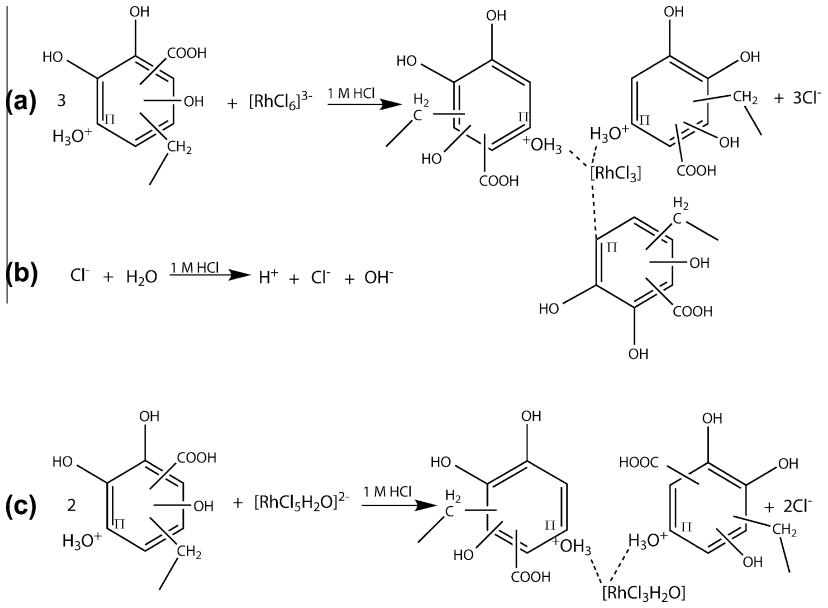


**Fig. 10.** Adsorption mechanism of Rh (III) species: (a) $[RhCl_6]^{3-}$ and (c) $[RhCl_5H_2O]^{2-}$ surface complex formation with protonated π carbons of TAR, (b) side reaction in the bulk solution occurs between $Cl^-$ and $H_2O$ to form $OH^-$ ions. The $H^+$ ion adsorbs competitively.

π sites decreases the Lewis basicity of the carbons to form C—$H_3O^+$ (Lewis-type acidic active site) due to an electron withdrawing effect which destroys the electron delocalization [99]. After realized adsorption, XRD pattern in Fig. 8 shows an amorphous structure which proves Rh (III) complexes have not reduced to its metallic form [72,46,73,8].

## 4. Conclusions

The ultimate purpose is to produce novel resin, and understanding how interactions between resin and PGM. For this purpose, valonea tannin–formaldehyde resol type condensation has been studied. TAR characterization done by using FTIR, SEM instruments. TAR particles, which are obtained by the condensation reaction between formaldehyde and tannin, do not dissolve in water, whereas the tannin dissolves in water. In order to represent PGM, two metal which bearing different chemical properties Pd (II), and Rh (III) were used. The adsorption capacity of TAR particles with respect to Pd (II), and Rh (III) were determined as 87.10, and 10.86 mg/g, respectively. For the recovery of PGM, the results obtained herein show that TAR particles can be used as an effective adsorbent from aqueous solution. The adsorption of Pd (II) and Rh (III) species onto TAR can occur via different steps and mechanisms.

It was found that Pd (II) was adsorbed onto the TAR particles as a reduced metallic Pd through redox reaction mechanism: chloropalladium (II) species were reduced to Pd (0), while hydroxyl groups of TAR were oxidized during the adsorption. The adsorption process can be divided into two steps: fast adsorption by the ligand substitution at the initial stage and slow adsorption by the subsequent redox reaction after the ligand substitution reaches an equilibrium state.

TAR particles were used as adsorbent for the removal of Rh (III) ions from 1 M HCl solutions. Rh (III) species $[RhCl_5H_2O]^{2-}$ and $[RhCl_2(H_2O)_4]^-$ are adsorbed onto polyphenol resin surface. Surface exchange and complexation as possible adsorption mechanisms were proposed and discussed meanwhile, reduction of Rh (III) species to metallic form do not occur in under these conditions. Obtained TAR was characterized by FTIR spectroscopy before and after adsorption of rhodium metal ions. Ideas are supported by the EDX, XRD, FTIR spectra and stoichiometrically. Adsorption kinetic, equilibrium isotherm, thermodynamics and system design can be examined in next studies.

The results suggest that GAR particles are very useful as an adsorbent in a novel recovery system for PGMs. For the recovery of Pd (II), and Rh (III), GAR adsorbent is quite an effective way to achieve a series of unit operations (extraction, reduction, adsorption, solid–liquid separation) simultaneously onto the GAR, and there is a little secondary waste (non-additives for reduction and precipitation). Therefore, this system shows good promise as a recovery method for PGMs. It is expected that not only the efficient Pd (II) and Rh (III) adsorption, but also the separation from the mixture of metal ions will be possible using GAR particles by controlling the solution composition (pH, pCl, ionic strength and distribution of PGM species).

## Appendix A. Supplementary material

Supplementary data associated with this article can be found, in the online version, at http://dx.doi.org/10.1016/j.cej.2013.01.043.

## References

[1] B. Godlewska-Zylkiewicz, Biosorption of platinum and palladium for their separation/preconcentration prior to graphite furnace atomic absorption spectrometric determination, Spectrochim. Acta B 58 (2003) 1531–1540.
[2] M. Goto, H. Kasaini, S. Furusaki, Selective separation of Pd(II), Rh(III), and Ru(III) ions from a mixed chloride solution using activated carbon pellets, Sep. Sci. Technol. 35 (2000) 1307–1327.
[3] M.S. Alam, K. Inoue, K. Yoshizuka, H. Ishibashi, Adsorptive separation of rhodium(lll) using Fe(lll)-templated oxine type of chemically modified chitosan, Sep. Sci. Technol. 33 (1998) 655–666.
[4] H. Kawakita, M. Abe, J. Inoue, K. Ohto, H. Harada, K. Inoue, Selective gold recovery using orange waste, Sep. Sci. Technol. 44 (2009) 2797–2805.
[5] D. Parajuli, H. Kawakita, K. Kajiyama, K. Ohto, H. Harada, K. Inoue, Recovery of gold from hydrochloric acid by using lemon peel gel, Sep. Sci. Technol. 43 (2008) 2363–2374.
[6] K. Hamamoto, H. Kawakita, K. Ohto, K. Inoue, Polymerization of phenol derivatives by the reduction of gold ions to gold metal, React. Funct. Polym. 69 (2009) 694–697.
[7] M. Goto, H. Kasaini, S. Furusaki, Adsorption performance of activated carbon pellets immobilized with organophosphorus extractants and an amine: A case study for the separation of Pt(IV), Pd(II), and Rh(III) ions in chloride media, Sep. Sci. Technol. 36 (2001) 2845–2861.

[8] K.F. Lam, C.M. Fong, K.L. Yeung, Separation of precious metals using selective mesoporous adsorbents, Gold Bull. 40 (2007) 192–198.
[9] H. Ma, X. Liao, X. Liu, B. Shi, Recovery of platinum(IV) and palladium(II) by bayberry tannin immobilized collagen fiber membrane from water solution, J. Membr. Sci. 278 (2006) 373–380.
[10] K. Khanbabaee, R.V. Ree, Tannins: classification and definition, Nat. Prod. Rep. 18 (2001) 641–649.
[11] S.H. McArt, D.E. Spalinger, J.M. Kennish, W.B. Collins, A modified method for determining tannin-protein precipitation capacity using accelerated solvent extraction (ASE) and microplate gel filtration, J. Chem. Ecol. 32 (2006) 1367–1377.
[12] M. Can, Adsorption of Palladium and Rhodium onto Polyphenol–Formaldehyde Resins, PhD Thesis; Institute of Science and Technology, Sakarya University, Sakarya, Turkey, 2011.
[13] R.W. Hemingway, P.E. Laks, Plant Polyphenols, Plenum Press, New York, 1992.
[14] E. Haslam, Natural polyphenols (vegetable tannins) as drugs: possible modes of action, J. Nat. Prod. 59 (1996) 205.
[15] L.-G. Chen, L.-L. Yang, K.-Y. Yen, T. Hatano, T. Yoshida, T. Okuda, Tannins of euphorbiaceous plants. XIII. New hydrolyzable tannins having phloroglucinol residue from glochidion rubrum BLUME, Chem. Pharm. Bull. 43 (1995) 2088–2090.
[16] J.-P. Salminen, M. Karonen, Chemical ecology of tannins and other phenolics: we need a change in approach, Funct. Ecol. 25 (2011) 325–338.
[17] G. Waghorn, W. McNabb, Consequences of plant phenolic compounds for productivity and health of ruminants, Proc. Nutr. Soc. 62 (2003) 383–392.
[18] I. Mueller-Harvey, Analysis of hydrolysable tannins, Anim. Feed Sci. Technol. 91 (2001) 3–20.
[19] B. Shi, Q. He, K. Yao, W. Huang, Q. Li, Production of ellagic acid from degradation of valonea tannins by *Aspergillus niger* and *Candida utilis*, J. Appl. Chem. Biotechnol. 90 (2005) 1154–1159.
[20] H. Özgünay, Ö. Sarı, M. Tozan, Molecular investigation of valonea tannin, J. Am. Leather Chem. Assoc. 102 (2007) 154–157.
[21] J. Handique, J. Baruah, Polyphenolic compounds: an overview, React. Funct. Polym. 52 (2002) 163–188.
[22] Turkish Standarts. Palamut Özü (Valeks); Türk Standartları Enstitüsü: Ankara, 1988.
[23] Turkish Standarts, Palamut ve Palamut Tırnakları, Türk Standartları Enstitüsü, Ankara, 1975
[24] H. Pasch, A. Pizzi, Considerations on the macromolecular structure of chestnut ellagitannins by matrix-assisted laser desorption/ionization-time-of-flight mass spectrometry, J. Appl. Polym. Sci. 85 (2002) 429–437.
[25] J. Jankun, S.H. Selman, R. Swiercz, E. Skrzypczak-Jankun, Why drinking green tea could prevent cancer, Nature 387 (1997) 561.
[26] S. Kim, H.J. Kim, Curing behavior and viscoelastic properties of pine and wattle tannin-based adhesives studied by dynamic mechanical thermal analysis and FT-IR–ATR spectroscopy, J. Adhes. Sci. Technol. 17 (2003) 1369–1383.
[27] J.M. Garro-Galvez, M. Fechtal, S. Riedl, Gallic acid as a model of tannins in condensation with formaldehyde, Thermochim. Acta 274 (1995) 149–163.
[28] W. Hesse, J. Lang, Phenolic Resins; Ullmann's Encyclopedia of Industrial Chemistry, Wiley-VCH, Wiesbaden, Germany, 2004.
[29] L. Pilato, J. Koo, G. Wissler, S. Lao, A review – Phenolic and related resins and their nanomodification into phenolic resin FRP systems, J. Adv. Mater. (Covina, CA, US) 40 (2008) 5–16.
[30] B. Adams, E. Holmes, Absorptive properties of synthetic resins: Part I, J. Soc. Chem. Ind. 54 (1935) 1T–9T.
[31] V.C. Malshe, E.S. Sujatha, Phenol based resin as alkylation catalyst, React. Funct. Polym. 43 (2000) 183–194.
[32] V. Strelko, M. Streat, O. Kozynchenko, Preparation, characterisation and sorptive properties of polymer based phosphorus-containing carbon, React. Funct. Polym. 41 (1999) 245–253.
[33] V. Gorshkov, V. Ivanov, I. Staina, Selectivity of phenol–formaldehyde resins and separation of rare alkali metals, React. Funct. Polym. 38 (1998) 157–176.
[34] J.L. Santana, L. Lima, J. Torres, F. Martínez, S. Olivares, Simultaneous metal adsorption on tannin resins, J. Radioanal. Nucl. Chem. 251 (2002) 467–471.
[35] K. Inoue, H. Kawakita, K. Ohto, T. Oshima, Adsorptive removal of uranium and thorium with a crosslinked persimmon peel gel, J. Radioanal. Nucl. Chem. 267 (2006) 435–442.
[36] X. Liao, H. Ma, R. Wang, B. Shi, Adsorption of $UO_2^{2+}$ on tannins immobilized collagen fiber membrane, J. Membr. Sci. 243 (2004) 235–241.
[37] X. Liao, L. Li, B. Shi, Adsorption recovery of thorium(IV) by *Myrica rubra* tannin and larch tannin immobilized onto collagen fibres, J. Radioanal. Nucl. Chem. 260 (2004) 619–625.
[38] T. Matsumura, S. Usuda, Applicability of insoluble tannin to treatment of waste containing americium, J. Alloy. Compd. 271 (1998) 244–247.
[39] M. McDonald, I. Mila, A. Scalbert, Precipitation of metal ions by plant polyphenols: optimal conditions and origin of precipitation, J. Agr. Food Chem. 44 (1996) 599–606.
[40] A. Şengil, M. Özacar, Biosorption of Cu(II) from aqueous solutions by mimosa tannin gel, J. Hazard. Mater. 157 (2008) 277–285.
[41] M. Özacar, İ.A. Şengil, H. Türkmenler, Equilibrium and kinetic data, and adsorption mechanism for adsorption of lead onto valonia tannin resin, Chem. Eng. J. 143 (2008) 32–42.
[42] H. Yu, G.H. Covey, A.J. O'Connor, Innovative use of silvichemical biomass and its derivatives for heavy metal sorption from wastewater, Int. J. Environ. Pollut. 34 (2008) 427–450.
[43] X. Huang, X. Liao, B. Shi, Hg(II) removal from aqueous solution by bayberry tannin-immobilized collagen fiber, J. Hazard. Mater. 170 (2009) 1141–1148.
[44] A. Nakajima, Y. Baba, Mechanism of hexavalent chromium adsorption by persimmon tannin gel, Water Res. 38 (2004) 2859–2864.
[45] Y. Nakano, T. Ogata, Y.H. Kim, Selective recovery process for gold utilizing a functional gel derived from natural condensed tannin, J. Chem. Eng. Jpn. 40 (2007) 270–274.
[46] R. Wang, X. Liao, B. Shi, Adsorption behaviors of Pt(II) and Pd(II) on collagen fiber immobilized bayberry tannin, Ind. Eng. Chem. Res. 44 (2005) 4221–4226.
[47] T. Ogata, Y. Nakano, Mechanisms of gold recovery from aqueous solutions using a novel tannin gel adsorbent synthesized from natural condensed tannin, Water Res. 39 (2005) 4281–4286.
[48] M. Can, E. Bulut, M. Özacar, Synthesis and characterization of gallic acid resin and its interaction with palladium(II), rhodium(III) chloro complexes, Ind. Eng. Chem. Res. 51 (2012) 6052–6063.
[49] J.M. Garro-Galvez, B. Riedl, Pyrogallol–formaldehyde thermosetting adhesives, J. Appl. Polym. Sci. 65 (1997) 399–408.
[50] Y. Xiong, C.R. Adhikari, H. Kawakita, K. Ohto, K. Inoue, H. Harada, Selective recovery of precious metals by persimmon waste chemically modified with dimethylamine, Bioresour. Technol. 100 (2009) 4083–4089.
[51] H. Kawakita, K. Hamamoto, K. Ohto, K. Inoue, Polyphenol polymerization by horseradish peroxidase for metal adsorption studies, Ind. Eng. Chem. Res. 48 (2009) 4440–4444.
[52] T. Holopainen, L. Alvila, J. Rainio, T.T. Pakkanen, IR spectroscopy as a quantitative and predictive analysis method of phenol–formaldehyde resol resins, J. Appl. Polym. Sci. 69 (1998) 2175–2185.
[53] H. Kawakita, R. Yamauchi, D. Parajuli, K. Ohto, H. Harada, K. Inoue, Recovery of gold from hydrochloric acid by means of selective coagulation with persimmon extract, Sep. Sci. Technol. 43 (2008) 2375–2385.
[54] D. Parajuli, H. Kawakita, K. Inoue, K. Ohto, K. Kajiyama, Persimmon peel gel for the selective recovery of gold, Hydrometallurgy 87 (2007) 133–139.
[55] W. Wang, L. Perng, G. Hsiue, F. Chang, Characterization and properties of new silicone-containing epoxy resin, Polymer 41 (2000) 6113–6122.
[56] V.L. Singleton, R. Orthofer, R.M. Lamuela-Raventós, Analysis of totalphenols and otheroxidationsubstrates and antioxidants by means of folin–ciocalteu reagent, Methods Enzymol. 299 (1999) 152–178.
[57] P.W. Hartzfeld, R. Forkner, M.D. Hunter, A.E. Hagerman, Determination of hydrolyzable tannins (gallotannins and ellagitannins) after reaction with potassium iodate, J. Agric. Food Chem. 50 (2002) 1785–1790.
[58] I. Poljanšek, M. Krajnc, Characterization of phenol–formaldehyde prepolymer resins by in line FT-IR spectroscopy, Acta Chim. Slov. 52 (2005) 238–244.
[59] A.L. Myers, Thermodynamics of adsorption in porous materials, AIChE J. 48 (2002) 145–160.
[60] J.-M. Raquez, M. Deléglise, M.-F. Lacrampe, P. Krawczak, Thermosetting (bio)materials derived from renewable resources: a critical review, Prog. Polym. Sci. 35 (2010) 487–509.
[61] C. Peña, M. Larrañaga, N. Gabilondo, A. Tejado, J.M. Echeverria, I. Mondragon, Synthesis and characterization of phenolic novolacs, J. Appl. Polym. Sci. 100 (2006) 4412–4419.
[62] R.M. Silverstein, F.X. Webster, Infrared spectrometry, in: Spectrometric Identification of Organic Compounds, sixth ed., Wiley, New York, 1998, pp. 90–138.
[63] R.O. Ebewele, B.H. River, J.A. Koutsky, Relationship between phenolic adhesive chemistry and adhesive joint performance: effect of filler type on fraction energy, J. Appl. Polym. Sci. 31 (1986) 2275–2302.
[64] I. Mohammed-Ziegler, F. Billes, Vibrational spectroscopic calculations on pyrogallol and gallic acid, J. Mol. Struct. – Theochem 618 (2002) 259–265.
[65] J. Lin, Q. Yang, X. Wen, Z.-Q. Cai, P. Pi, J. Cheng, Z. Yang, Synthesis and characterization of phenolic novolacs modified by chestnut and mimosa tannin extracts, J. Polym. Res. 18 (2011) 1667–1677.
[66] Y.K. Lee, H.J. Kim, M. Rafailovich, J. Sokolov, Curing monitoring of phenolic resol resins via atomic force microscope and contact angle, Int. J. Adhes. Adhes. 22 (2002) 375–384.
[67] G. Keresztury, F. Billes, M. Kubinyi, T. Sundius, A density functional, infrared linear dichroism, and normal coordinate study of phenol and its deuterated derivatives: revised interpretation of the vibrational spectra, J. Phys. Chem. 102 (1998) 1371–1380.
[68] I. Poljansek, U. Sebenik, M. Krajnc, Characterization of phenol–urea–formaldehyde resin by inline FTIR spectroscopy, J. Appl. Polym. Sci. 99 (2006) 2016–2028.
[69] M.H. Choi, H.Y. Byun, I.J. Chung, The effect of chain length of flexible diacid on morphology and mechanical property of modified phenolic resin, Polymer 43 (2002) 4437–4444.
[70] S. Arasaretnam, L. Karunanayake, Synthesis, characterization, and metal adsorption properties of tannin–phenol–formaldehyde resins produced using tannin from dried fruit of *Terminalia chebula* (Aralu), J. Appl. Polym. Sci. 115 (2010) 1081–1088.
[71] C.R. Adhikari, D. Parajuli, K. Inoue, K. Ohto, H. Kawakita, H. Harada, Recovery of precious metals by using chemically modified waste paper, New J. Chem. 32 (2008) 1634–1641.
[72] M.A. Abidin, A.A. Jalil, S. Triwahyono, S.H. Adama, N.N. Kamarudin, Recovery of gold(III) from an aqueous solution onto a durio zibethinus husk, Biochem. Eng. J. 54 (2011) 124–131.
[73] Y.H. Kim, Y. Nakano, Adsorption mechanism of palladium by redox within condensed-tannin gel, Water Res. 39 (2005) 1324–1330.

[74] M. Ruiz, A.M. Sastre, E. Guibalc, Palladium sorption on glutaraldehyde-crosslinked chitosan, React. Funct. Polym. 45 (2000) 155–173.
[75] I. Puigdomenech, Hydra and Medusa, Version, 2010. <http://www.kemi.kth.se/medusa/>.
[76] A. Uheida, M. Iglesias, C. Fontàs, Y. Zhang, M. Muhammed, Adsorption behavior of platinum group metals (Pd, Pt, Rh) on nonylthiourea-coated $Fe_3O_4$ nanoparticles, Sep. Sci. Technol. 41 (2006) 909–923.
[77] W.J. Gerber, K.R. Koch, H.E. Rohwer, E.C. Hosten, T.E. Geswindt, Separation and quantification of $[RhCln(H_2O)6-n]3-n$ $(n = 0–6)$ complexes, including stereoisomers, by means of ion-pair HPLC–ICP-MS, Talanta 82 (2010) 348–358.
[78] V. Salvado, J.M. Sanchez, M. Hidalgo, J. Havel, The speciation of rhodium(III) in hydrochloric acid media by capillary zone electrophoresis, Talanta 56 (2002) 1061–1071.
[79] D. Pletcher, R.I. Urbina, Electrodeposition of rhodium. Part 1. Chloride solutions, J. Electroanal. Chem. 42 (1997) 137–144.
[80] E. Piron, M. Accominotti, A. Domard, Interaction between chitosan and uranyl ions. Role of physical and physicochemical parameters on the kinetics of sorption, Langmuir 13 (1997) 1653–1658.
[81] S.S. Aleksenko, A.P. Gumenyuk, S.P. Mushtakova, A.R. Timerbaev, Speciation studies by capillary electrophoresis – distribution of rhodium(III) complexed forms in acidic media, Fresenius J. Anal. Chem. 370 (2001) 865–871.
[82] M. Can, E. Bulut, M. Özacar, Synthesis and characterization of pyrogallol–formaldehyde nano-resin and its usage as adsorbent, J. Chem. Eng. Data 57 (2012) 2710–2717.
[83] A. Uheida, M. Iglesias, C. Fontàs, M. Hidalgo, V. Salvadó, Sorption of palladium(II), rhodium(III), and platinum(IV) on $Fe_3O_4$ nanoparticles, J. Colloid Interface Sci. 301 (2006) 402–408.
[84] R. Li, Q. Hea, Z. Hua, S. Zhanga, L. Zhang, X. Changa, Highly selective solid-phase extraction of trace Pd(II) by murexide functionalized halloysite nanotubes, Anal. Chim. Acta 713 (2012) 136–144.
[85] Y. Liu, J. Fu, R. Li, X. Zhang, Z. Hu, Studies on biosorption of $Pd^{2+}$ by bacteria, Acta Microbiol. Sin. 40 (2000) 535–539.
[86] C.L. Mack, B. Wilhelmi, J.R. Duncan, J.E. Burgess, Biosorptive recovery of platinum from platinum group metal refining wastewaters by immobilised *Saccharomyces cerevisiae*, Water Sci. Technol. 63 (2010) 149–155.
[87] Z. Tu, S. Lu, X. Chang, Z. Li, Z. Hu, L. Zhang, H. Tian, Selective solid-phase extraction and separation of trace gold, palladium and platinum using activated carbon modified with ethyl-3-(2-aminoethylamino)-2-chlorobut-2-enoate, Microchim. Acta 173 (2011) 231–239.
[88] J. Park, S.W. Won, J. Mao, I.S. Kwak, Y.-S. Yun, Recovery of Pd(II) from hydrochloric solution using polyallylamine hydrochloride-modified *Escherichia coli* biomass, J. Hazard. Mater. 181 (2010) 794–800.
[89] P. Ramakul, Y. Yanachawakul, N. Leepipatpiboon, N. Sunsandee, Biosorption of palladium(II) and platinum(IV) from aqueous solution using tannin from Indian almond (*Terminalia catappa* L.) leaf biomass: kinetic and equilibrium studies, Chem. Eng. J. 193–194 (2012) 102–111.
[90] A. Sari, D. Mendil, M. Tuzen, M. Soylak, Biosorption of palladium(II) from aqueous solution by moss (Racomitrium lanuginosum) biomass: equilibrium, kinetic and thermodynamic studies, J. Hazard. Mater. 162 (2009) 874–879.
[91] E. Guibal, N.V.O. Sweeney, T. Vincent, J. Tobin, Sulfur derivatives of chitosan for palladium sorption, React. Funct. Polym. 50 (2002) 149–163.
[92] A. Ramesh, H. Hasegawa, W. Sugimoto, T. Maki, K. Ueda, Adsorption of gold(III), platinum(IV) and palladium(II) onto glycine modified crosslinked chitosan resin, Bioresour. Technol. 99 (2008) 3801–3809.
[93] K. Fujiwara, A. Ramesh, T. Maki, H. Hasegawa, K. Ueda, Adsorption of platinum (IV), palladium (II) and gold (III) from aqueous solutions onto l-lysine modified crosslinked chitosan resin, J. Hazard. Mater. 146 (2007) 39–50.
[94] F. Li, C. Bao, J. Zhang, Z. An, W. Kong, H.W.Y. Liu, L. Wang, Sorption technique for the determination of trace palladium in geological samples using atomic absorption spectrometry, Anal. Lett. 43 (2010) 1857–1868.
[95] L. Zhou, J. Liu, Z. Liu, Adsorption of platinum(IV) and palladium(II) from aqueous solution by thiourea-modified chitosan microspheres, J. Hazard. Mater. 172 (2009) 439–446.
[96] D. Parajuli, K. Hirota, K. Inoue, Trimethylamine-modified lignophenol for the recovery of precious metals, Ind. Eng. Chem. Res. 48 (2009) 10163–10168.
[97] P.J.M. Carrott, M.M.L.R. Carrott, A.J.E. Candeias, J.P.P. Ramalho, Numerical Simulation of surface ionisation and specific adsorption on a two-site model of a carbon surface, J. Chem. Soc., Faraday Trans. 91 (1995) 2179–2184.
[98] B. Côté, G.P. Demopoulos, New 8-hydroxyquinoline derivative extractants for platinum group metals separation Part 4: kinetics of Pd(II) extraction and stripping, Solvent Extr. Ion Exch. 13 (1995) 83–107.
[99] R.-L. Jia, C.-Y. Wang, S.-M. Wang, Preparation of carbon supported platinum catalysts: role of π sites on carbon support surface, J. Mater. Sci. 41 (2006) 6881–6888.